Phase transitions in the fully frustrated XY model studied with use of the microcanonical Monte Carlo technique

Sooyeul Lee and Koo-Chul Lee
Department of Physics and Center for Theoretical Physics, Seoul National University, Seoul 151-742, Korea
(Received 20 December 1993)

We investigate the phase transitions of the frustrated XY model in the square lattice with frustration parameter $f = \frac{1}{2}$. The system has doubly degenerate ground states in addition to those associated with U(1) symmetry. We study the system via a high-precision Monte Carlo technique. It is found that the system has two separate transitions. At the lower temperature $0.440(2)J/k_B$, we find a Kosterlitz-Thouless transition with a larger-than-universal jump in the helicity modulus. The critical index $\eta(T_{KT})$ of the spin-spin correlation function is 0.220(2), less than the universal value of $\frac{1}{4}$. At higher temperature $0.454(2)J/k_B$, we find a second-order vortex-lattice melting transition with critical indices $\alpha = 0.363(10)$, $\beta = 0.089(8)$, $\gamma = 1.448(24)$, and $\nu = 0.813(5)$.

I. INTRODUCTION

Over the past ten years, two dimensional (2D) fully frustrated XY (FFXY) models have been the subject of intense investigation, both numerically and analytically.[1-7] For the square lattice, the FFXY model has a continuous U(1) symmetry, corresponding to global rotation of the spins, and a discrete Z_2 symmetry, corresponding to long-range order of the ground state vortex lattice. In the ground state, the vortices, which show up as charges $\pm\frac{1}{2}$ on the sites of the dual lattice, are ordered in a checkerboard pattern. The ground state, besides global rotations, has twofold degeneracy, corresponding to the degeneracy of the antiferromagnetic Ising (AFI) model. Due to these continuous and discrete symmetries of the ground states of the model, two kinds of phase transitions are possible. Associated with U(1) symmetry, vortex excitations may appear as a mechanism of the Kosterlitz-Thouless (KT) transition.[8] In this case the helicity modulus, which measures quasi-long-range order related to the continuous U(1) symmetry, has a discontinuous jump at the KT transition temperature:[9] In the frustrated XY model the jump size can be larger than the universal value of the usual XY model.[10] In view of the Z_2 symmetry of the ground states, domain-wall excitations between the two different antiferromagnetic phases appear as a mechanism of the continuous vortex-lattice melting transition. The fluctuation of domain walls diverges at the vortex melting transition point and thus the specific heat peak, a sign of long-range order of the chirality associated with the discrete symmetry, diverges at the same point. Though there are some similarities between the AFI model and the FFXY model, the critical behaviors of the vortex melting transition can be different from those of the true Ising transition because the similarities are based only on symmetry of the ground state configurations and interaction between different domains is highly complex, unlike in the Ising model.

There are two possible scenarios of phase transitions in the FFXY model. One is simultaneous occurrence of KT and vortex melting transitions. The other is separate occurrence of the two, in a decoupled fashion of domain-wall and vortex excitations. There have been several analytical and numerical studies[2-7] on the FFXY model in the square lattice since the work of Teitel and Jayaprakash.[1] But it is still unsettled whether the FFXY model has a single transition or double transitions. Monte Carlo (MC) simulations of the FFXY model show a single transition. Nicolaides[2] has studied Ising and XY correlation functions in the FFXY model and found simultaneous occurrence of Ising and KT transitions. Lee *et al.*[3] have also studied the FFXY model and asserted a single transition with non-Ising critical behaviors, based on an analysis of Ising-like order parameter only. Recently, Ramirez-Santiago and José[4] have investigated the FFXY model using analyses of U(1) and Z_2 gauge-invariant correlation functions. They found a KT transition with nonuniversal KT jump and a vortex melting transition with non-Ising critical behaviors at the same temperature as the KT transition. On the other hand, some MC results of the Coulomb gas (CG) with half integer charges, which is believed to be in the same universality class as the FFXY model,[11] show two separate transitions. Grest[5] has found two separate Ising and KT transitions, with a nonuniversal KT jump. Recently, Lee[6] has also found two separate transitions: The lower is the KT transition with a larger-than-universal KT jump and the upper is the vortex melting transition with non-Ising critical behaviors.

From the MC results of the CG with half integer charges, we know that the separation of possible double transitions is very small. As a necessity, it needs a high-precision Monte Carlo technique to investigate phase transition(s) of the FFXY model. We thus adopt a technique found by Lee,[12] which is powerful in a system with discrete energy like the Ising model. We modify the technique suitably for the continuous FFXY model.

In order to determine whether the model has a single

or double transition, we measure thermodynamic quantities related to KT and vortex melting transition independently. For the KT transition, the helicity modulus and XY susceptibility are measured; for the vortex melting transition, specific heat, staggered magnetization of vortex charges, and susceptibility of the staggered magnetization are measured. We then adopt several finite-size-scaling analyses to estimate transition temperatures and determine critical behaviors. As a result we find double transitions. At lower temperature $0.440(2)J/k_B$, we find a KT transition with a larger-than-universal jump in the helicity modulus. At higher temperature $0.454(2)J/k_B$, we find a second-order vortex-lattice melting transition, whose scaling behavior is different from that of the 2D Ising model.

In the following section, we will give a brief explanation of our Monte Carlo technique and discuss several finite-size-scaling methods used for data analysis. In Sec. III, we will show the data of the MC simulations and give those scaling results.

II. METHODS OF ANALYSIS

Uniformly frustrated XY models are defined by a nearest-neighbor Hamiltonian

$$H = -\sum_{\langle i,j \rangle} J\cos(\theta_i - \theta_j - A_{ij}) \tag{1}$$

with

$$A_{ij} = \frac{2\pi}{\Phi_0}\int_i^j \mathbf{A}\cdot d\mathbf{r},$$

where θ_i is the phase of the spin at the ith site, $\Phi_0 \equiv hc/2e$ is the magnetic flux quantum, $\mathbf{A}$ is the vector potential due to the external transverse magnetic field $\mathbf{B}$, and J is the coupling strength between neighboring spins. In the case of the FFXY model the directed sum around a unit plaquette $\sum A_{ij} = \pi$.

In order to apply our MC technique to the FFXY model with continuous energy spectrum, we divide the continuous energy into many uniform intervals. We replace the intervals with their mean values and thus make the energy of the system discrete. The canonical average $\langle A\rangle$ of any thermodynamic quantity A is defined by

$$\langle A\rangle = \frac{\sum_E \Omega(E)A(E)\exp(-\beta E)}{\sum_E \Omega(E)\exp(-\beta E)}\ , \tag{2}$$

where E is the mean energy of a given interval, $\Omega(E)$ is the number of states in the interval, and $A(E)$ is the microcanonical average of A in the interval. As all the $\Omega(E)$'s are infinite we measure their relative ratios in the MC simulation. In the simulation, $A(E)$ and the relative ratio of neighboring $\Omega(E)$'s are measured. The inverse temperature β is a continuous parameter used for calculation of the canonical average. With the aid of the above method we calculate several thermodynamic quantities as a continuous function of β.

In the ground states of the FFXY model on a square lattice, vortex charges are ordered in a checkerboard pattern. In view of the similarity between the ground states of the FFXY model and the AFI model, we introduce a staggered magnetization, which we consider as an Ising-like order parameter, as follows

$$M = \frac{1}{L^2}\left|\sum_i 2m(\mathbf{r}_i)(-1)^{x_i+y_i}\right|\ , \tag{3}$$

where $m(\mathbf{r}_i)$ is a vortex charge on the sites of the dual lattice and L is the linear size of the system. The $m(\mathbf{r}_i)$ is calculated using local chirality as follows

$$m(\mathbf{r}_i) = \frac{1}{2\pi}\sum(\theta_i - \theta_j - A_{ij})\ , \tag{4}$$

where $|\theta_i - \theta_j - A_{ij}| \le \pi$ and the sum is a directed one around a unit plaquette. From the MC simulation it is found that the $m(\mathbf{r}_i)$ has only $\pm\frac{1}{2}$ values near the transition temperature or below. According to the scaling hypothesis,[13] the free energy density $f \equiv -\frac{1}{N}\ln Z$ consists of the analytic part f_a and the singular part f_s, i.e., $f = f_a + f_s$. The singular part behaves as

$$f_s(t,h,L) = L^{-d}f_s(tL^{y_t}, hL^{y_h}). \tag{5}$$

In the above equation $t \equiv \frac{T-T_c}{T_c}$ and h are scaling fields and $y_t \equiv 1/\nu$ and $y_h \equiv d - \beta/\nu$ are the corresponding critical exponents. The scaling law of magnetization is given by

$$M = L^{-\beta/\nu}f_h^{(1)}(tL^{y_t}, 0), \tag{6}$$

where $f_h^{(1)}$ is the field derivative of f_s. The magnetic susceptibility $\chi_m(L) \equiv \frac{L^2}{k_BT}(\langle M^2\rangle - \langle M\rangle^2)$ has the following scaling equation at the point of its extremum:

$$\chi_m^{\max} = g_0 L^{\gamma/\nu}. \tag{7}$$

In order to determine critical behaviors and the transition temperature corresponding to the vortex melting transition, we do finite-size-scaling analyses of magnetic susceptibility, magnetization, and specific heat. We determine γ/ν by fitting maximum values of susceptibility to Eq. (7). As the transition temperature is yet unknown, it is necessary to obtain a profile of β/ν with respect to assumed transition temperatures by least squares fit of our magnetization data to Eq. (6). At the vortex melting transition temperature T_c, the hyperscaling relation between critical exponents, i.e., $d\nu = \gamma + 2\beta$, is satisfied. In this way, T_c and β/ν are estimated. To determine the critical exponent $1/\nu$, we use the dependence of the specific heat peak on the system size, $C_{\text{peak}} \sim L^{\alpha/\nu}$, and the hyperscaling relation, $\alpha = 2 - d\nu$. For another method to estimate T_c, we use following scaling relation. The difference between $T_{\max}(L)$, at which the specific heat of the lattice size L has a maximum value, and T_c is given by

$$T_{\max}(L) - T_c = x_0 L^{-1/\nu}\ , \tag{8}$$

where the exponent $1/\nu$ is the value obtained via the scal-

ing of the specific heat peak. As the transition temperature T_c is unknown, $1/\nu$ is calculated at several assumed T_c's by fitting the MC data of $T_{\max}(L)$ to Eq. (8). We regard the temperature where the exponent $1/\nu$ is consistent with the value obtained via the scaling of the specific heat peak as the transition temperature T_c. Equation (8) is also applied to the susceptibility. As a direct method to estimate T_c, we use an interesting quantity $P_L(T,M)$, the probability distribution of magnetization, which was introduced by Binder.[14] Here the function $P_L(T,M)$ is normalized such that $\int_{-\infty}^{+\infty} P_L(T,M)dM = 1$. We obtain $P_L(T,M=0)$ in several lattice sizes. Below the transition temperature T_c, the system tends to go to one of the two antiferromagnetic phases and thus $P_L(T)$ decreases to zero as system size L increases. Above T_c, however, $P_L(T)$ increases as system size L increases because the system tends to go to the disordered phase. Therefore, a common crossing point of $P_L(T)$ curves for different lattice sizes will appear. The common crossing point is the transition temperature according to the above arguments.

To determine critical behaviors and the transition temperature of the KT transition, we measure the helicity modulus and the XY susceptibility. The helicity modulus for the frustrated XY model is defined by

$$\Upsilon = -\frac{1}{2}\langle u\rangle - \frac{J}{k_B T L^2}\left\langle \left(\sum_{\langle i,j\rangle} \sin(\theta_i - \theta_j - A_{ij})x_{ij}\right)^2 \right\rangle \tag{9}$$

where $x_{ij} = x_i - x_j$ and $\langle u\rangle$ is the mean energy per spin. The XY susceptibility is defined as a sum of four sublattice susceptibilities in view of the ground state configurations of the FFXY model,[15]

$$\chi_{XY} = \frac{1}{4}\sum_{i=1}^{4}\chi^{(i)}, \tag{10}$$

where $\chi^{(i)}$ is the XY susceptibility of the ith sublattice. In the case of an unfrustrated XY model, the helicity modulus Υ has a discontinuous jump to zero at the KT transition temperature $T_{\rm KT}$. The jump size $\Upsilon(T_{\rm KT})/T_{\rm KT}$ has the universal value of $\frac{2}{\pi}$ according to Nelson and Kosterlitz's arguments.[9] In the FFXY model, the jump size is suggested to be larger than the universal value. Thus the crossing point between the universal jump line $\frac{2}{\pi}T$ and the helicity modulus of a lattice size L gives an upper bound for $T_{\rm KT}$. In the limit of large L, we can extrapolate a minimal upper bound, which gives a KT bound for $T_{\rm KT}$. For a different method to estimate another KT bound, we follow Minnhagen's argument.[16] He finds that the exponent η of the spin-spin correlation function has a nonuniversal value less than $\frac{1}{4}$ in the case of the frustrated XY model with a nonuniversal KT jump. Below the KT transition temperature, the spin-spin correlation function decays algebraically and thus the susceptibility diverges with the size of the system as

$$\chi_{XY}(L,T) \sim L^{2-\eta(T)}. \tag{11}$$

From MC data of $\chi_{XY}(L,T)$ for several lattice sizes we determine the exponent $\eta(T)$. We regard the temperature at which η is $\frac{1}{4}$ as another KT bound for $T_{\rm KT}$. As a more accurate method to estimate both $T_{\rm KT}$ and the jump size in the helicity modulus, we use Weber and Minnhagen's finite-size-scaling equations.[17] Introducing logarithmic corrections to the Kosterlitz recursion equations, they find

$$\Upsilon(T_{\rm KT},L) = \frac{2}{\pi}T^*_{\rm KT}\left(1 + \frac{1}{2}\frac{1}{\ln L + c}\right), \tag{12}$$

where $T^*_{\rm KT}$ and c are free parameters. $T^*_{\rm KT}$, related to the jump size, is equal to $T_{\rm KT}$ in the case of the usual XY model. We do a χ^2 fit of the MC data at various temperatures to Eq. (12). The transition temperature $T_{\rm KT}$ is the point at which fitting error is minimum. The fitted parameter $T^*_{\rm KT}$, at $T_{\rm KT}$, times $\frac{1}{T_{\rm KT}}$ gives the jump size in the helicity modulus Υ.

III. NUMERICAL RESULTS

We first consider the charge-lattice melting transition. In Fig. 1, we plot $\chi_m^{\max}(L)$, the maximal value of the magnetic susceptibility, on a log-log scale for lattice sizes from $L = 12$ to $L = 48$. We have performed six independent runs to obtain $\chi_m^{\max}(L)$ and $M(L,T)$. The data points of $\chi_m^{\max}(L)$ have good statistics as if they were on a straight line. From the slope of the data points and Eq. (7), we find $\gamma/\nu = 1.781(18)$. The hyperscaling relation, $d\nu = \gamma + 2\beta$, gives $\beta/\nu = 0.110(9)$. To determine T_c, where this hyperscaling relation is satisfied, we calculate β/ν at various assumed transition temperatures by fitting MC data to Eq. (6) with $t = 0$. In Table I, we find $T_c = 0.453(1)J/k_B$, where β/ν is consistent with the above value. In Fig. 2, we show the data for the specific heat peaks on a log-log scale for lattice sizes from $L = 12$ to $L = 64$. The average has been performed over 18 independent runs. The slope $\alpha/\nu = 0.459(16)$ for lattice sizes $L \geq 16$. From the hyperscaling relation $d\nu = 2 - \alpha$,

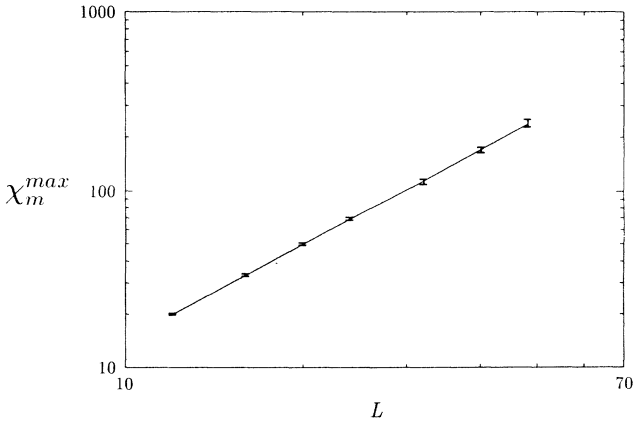

FIG. 1. Maximum values of magnetic susceptibility for lattice sizes $L = 12$, 16, 20, 24, 32, 40, and 48. The fitted value of γ/ν is 1.781(18). The solid line is a least χ^2 fit.

TABLE I. Estimation of exponents β/ν and $1/\nu$ at several assumed T_c's.

T_c (units of J/k_B) (Assumed)	β/ν (Magnetization)	$1/\nu$ (Specific heat)	$1/\nu$ (Susceptibility)
0.451	0.092(6)	0.886(25)	1.062(26)
0.452	0.102(6)	0.957(28)	1.119(30)
0.453	0.113(7)	1.043(34)	1.183(35)
0.454	0.125(7)	1.150(45)	1.256(43)
0.455	0.138(8)	1.289(63)	1.342(54)
0.456	0.152(8)	1.474(87)	1.443(69)

we find $1/\nu = 1.230(8)$. We also investigate the data on a semilog scale. However, the data points have a weak curvature and thus the possibility of an Ising transition with $\alpha = 0$ is ruled out. Applying Eq. (8), we calculate $1/\nu$ at various assumed transition temperatures in Table I. The transition temperature at which the value of $1/\nu$ is consistent with 1.230(8) obtained from the specific heat peak scaling is $0.455(1)J/k_B$ in the case of the specific heat and $0.454(1)J/k_B$ in the case of the susceptibility. As a direct method to estimate T_c, we plot $P_L(T)$ versus T for various lattice sizes L =16–48 (see Fig. 3). For each lattice size we have performed six independent runs to obtain $P_L(T)$. From the common intersection of the curves, we find $T_c = 0.454(2)J/k_B$, which is consistent with the previous results.

In order to determine the KT transition temperature, we measure a KT bound of $T_{\rm KT}$ from the helicity modulus. We obtain the helicity modulus for lattice sizes L =12–128 [see Fig. 4(a)]. Averaging has been performed over ten independent runs. In Fig. 4(b), we plot the intersection temperatures between the universal jump line $\frac{2}{\pi}T$ and the helicity modulus for lattice sizes L =20–128. Each intersection temperature is an upper bound of $T_{\rm KT}$ with given lattice size L. The intersection for the largest lattice size $L = 128$ is $0.449(1)J/k_B$. The rough estimate for the upper bound of $T_{\rm KT}$ is $0.447(1)J/k_B$ in the large L limit. In order to find another KT bound of $T_{\rm KT}$, we calculate the temperature-dependent exponent η of the spin-spin correlation function by fitting $\chi_{XY}(L,T)$ data to Eq. (11) (see Fig. 5). Following Minnhagen's argument, we can regard the temperature where η is $\frac{1}{4}$ as another KT bound, which we find is $0.444(1)J/k_B$. The error of the χ^2 fit becomes large as temperature increases. Especially, we find that the fitting error becomes noticeably large from $T \sim 0.444J/k_B$, which means that Eq. (11) does not hold above this temperature. Therefore we can regard $0.444J/k_B$ as a rough estimate of the KT transition temperature.

To determine both $T_{\rm KT}$ and the jump in the helicity modulus Υ, we apply Weber and Minnhagen's finite-size-scaling analysis. In Fig. 4(c), we plot the χ^2-fit errors, relative to the statistical uncertainties in the MC data, of the helicity modulus to the scaling form Eq. (12) for lattice sizes L =12–40. We find $T_{\rm KT} = 0.440(2)J/k_B$, at which the χ^2 error is minimum, $T^*_{\rm KT} = 0.504(12)J/k_B$, and $c = -0.818(70)$. The jump size in $\Upsilon(T_{\rm KT})/T_{\rm KT}$ is 1.15(3) times larger than the universal value of $\frac{2}{\pi}$. This value is compared with the results of Grest,[5] 1.22(8), and that of Lee,[6] 1.34. The jump size is sensitive to $T_{\rm KT}$ and increases rapidly as $T_{\rm KT}$ decreases. Weber and Minnhagen's finite-size-scaling equation is correct in the large L limit. However, the data fluctuation of the helicity modulus in a large system becomes so large that Weber and Minnhagen's scaling equation is not applicable. We thus use helicity modulus data up to lattice size $L = 40$, where MC data of the helicity modulus still have good statistics. In Fig. 4(d), we plot Weber

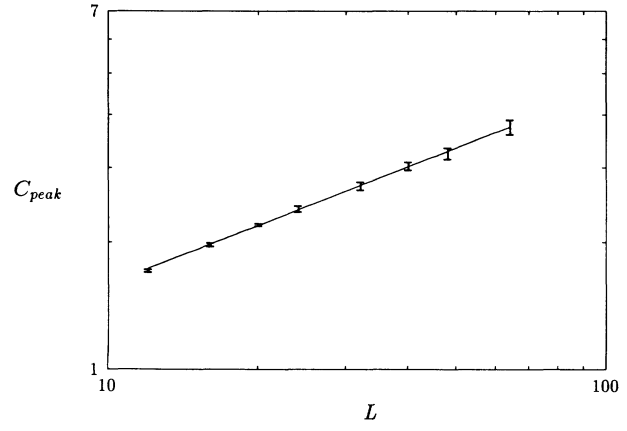

FIG. 2. Log-log plot of specific heat peak for lattice sizes L = 12, 16, 20, 24, 32, 40, 48, and 64. The fitted value of α/ν is 0.459(16) for lattice sizes $L \geq 16$. The solid line is a least χ^2 fit to $L \geq 16$.

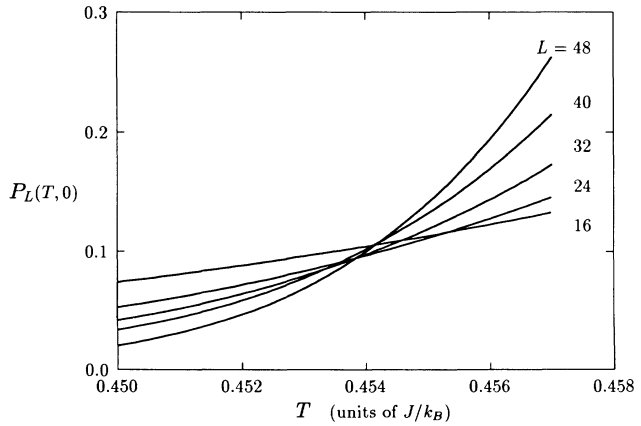

FIG. 3. Normalized probability distribution function $P_L(T, M = 0)$ for lattice sizes L = 16, 24, 32, 40, and 48. The common crossing point is about $0.454(2)J/k_B$.

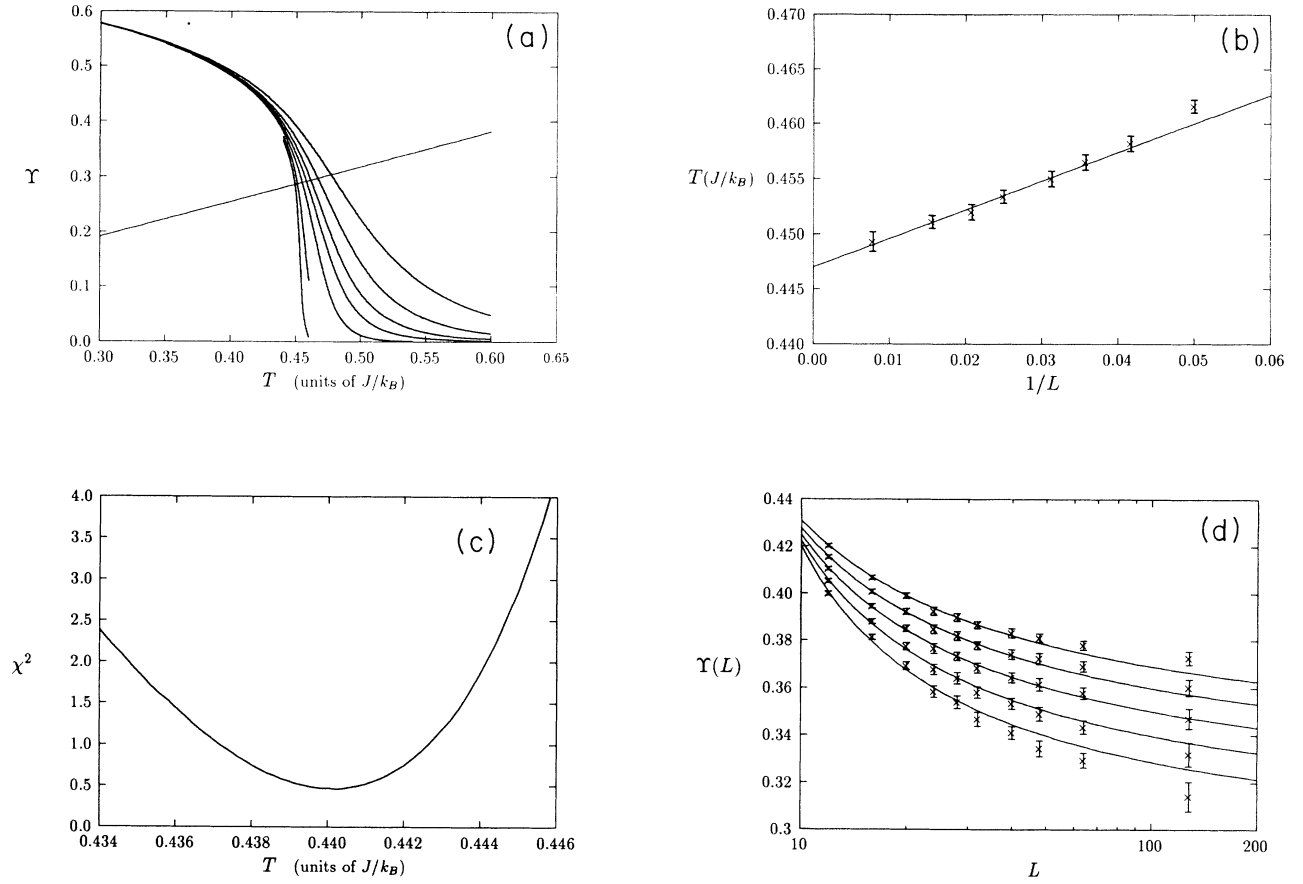

FIG. 4. (a) Helicity modulus of lattice sizes $L = 12, 16, 20, 24, 32, 64$, and 128. Each intersection with the line $\frac{2}{\pi}T$ gives an upper bound of the KT transition temperature. The error bars are hidden by the curves. (b) KT bound for lattice sizes $L = 20, 24, 28, 32, 40, 48, 64$, and 128. In the large L limit, the estimate for the upper bound of T_{KT} is $0.447J/k_B$. The line is merely a guide to the eyes. (c) χ^2-fit error, relative to the statistical uncertainties in the MC data, of helicity modulus data to Weber and Minnhagen's scaling equation. We use lattice sizes $L = 12, 16, 20, 24, 28, 32$, and 40. The temperature of minimum χ^2 error is $0.440(2)J/k_B$. (d) Weber and Minnhagen's scaling equation together with the MC data for lattice sizes $L = 12$–128. We use temperatures $T = 0.437, 0.439, 0.441, 0.443$, 0.445 from top to bottom. The best fit is for $T = 0.441J/k_B$.

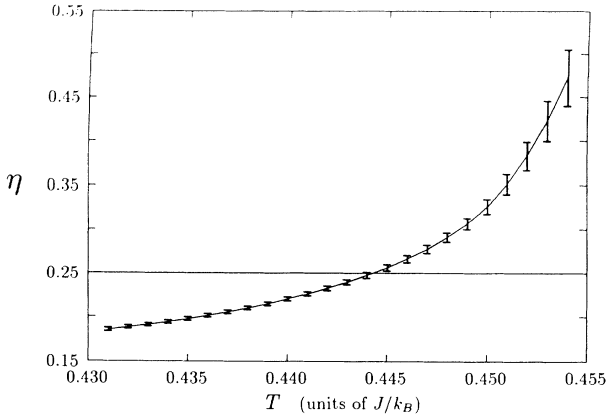

FIG. 5. Exponent η of spin-spin correlation function as a function of T. The KT upper bound, where $\eta = \frac{1}{4}$, is $0.444(1)J/k_B$. The fit error becomes large from $T \sim 0.444J/k_B$.

and Minnhagen's scaling equation together with the MC data at several temperatures for lattice sizes $L = 12$–128. At each temperature the scaling equation is obtained using the above χ^2 fit. As the system size becomes larger, all MC data, except when $T = 0.441J/k_B$, deviate from the corresponding scaling equation. This result confirms $T_{\mathrm{KT}} = 0.440(2)J/k_B$.

To check the results for the charge-lattice melting transition, we do scaling plots of several thermodynamic functions, which are calculable from derivatives of the free energy density (5). Following the scheme in Ref. 18, we denote the nth-order derivative of f with respect to ϵ by $\Gamma_n \equiv \frac{\partial^n f}{\partial \epsilon^n} = \frac{\partial^n f}{\partial(-K)^n}$, where ϵ is the temperature scaling field defined by $\epsilon = K_c - K$ and $K = \beta J$. The scaled temperature x can be written as $x = \epsilon L^{1/\nu}$. Now each derivative Γ_n is written as a sum of an analytical part Γ_{na} and a singular part Γ_{ns}, where $L^{d-\frac{n}{\nu}}\Gamma_{ns}(x)$ should collapse into the nth derivative of the scaling function $Y^{(n)}$ for all L. As the free energy density cannot

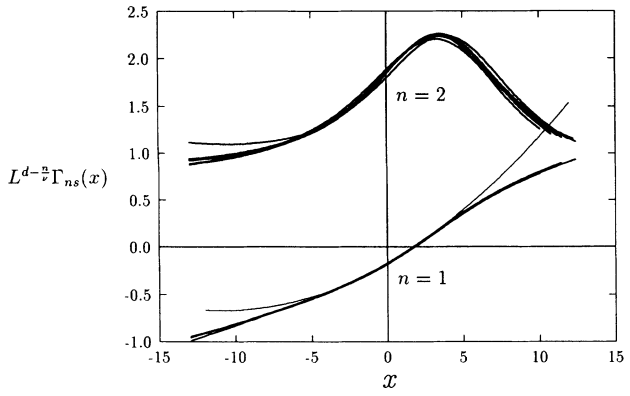

FIG. 6. $L^{d-\frac{n}{\nu}}\Gamma_{ns}(x)$ vs x for lattice sizes $L = 12, 16, 20, 24, 32, 40, 48$, and 64. (y_1, y_2) are $(-1.0, 2.5)$ and $(-0.05, 0.125)$ for $n = 1$, and 2, respectively. The curve tangent to $Y^{(n=1)}$ is the Taylor series approximation obtained in Sec. III.

be obtained in our MC technique we expand the analytical part of Γ_1 as $\Gamma_{1a} = \sum_{n=0}^{\infty} a_n \frac{\epsilon^n}{n!}$ and the singular part as $Y^{(1)} = \sum_{n=0}^{\infty} c_n \frac{x^n}{n!}$. Using the technique in Ref. 18, we obtain $L^{d-\frac{1}{\nu}}\Gamma_{1s}(x)$ and $L^{d-\frac{2}{\nu}}\Gamma_{2s}(x)$, where $K_c = \frac{1}{0.454}$ and $1/\nu = 1.230$ (see Fig. 6). They collapse nicely into single curves $Y^{(n)}$ for all L. We obtain $-1.0793(3), 0.027(8), 0.168(56)$ for a_n $(n = 0, 1, 2)$ and $-0.170(3), 0.092(2), 0.008(1)$ for c_n $(n = 0, 1, 2)$.

IV. CONCLUSION

We have studied the phase transitions in the fully frustrated XY model on a square lattice via a high-precision MC technique. It is found that the model has two separate transitions. The KT transition, at $0.440(2)J/k_B$, has a nonuniversal jump in the $\Upsilon(T_{\rm KT})/T_{\rm KT}$, $1.15(3)\frac{2}{\pi}$. The exponent $\eta(T_{\rm KT})$ of the spin-spin correlation function is 0.220(2), less than the universal value of $\frac{1}{4}$. At higher temperature, $T_c = 0.454(2)J/k_B$, we find a second-order charge-lattice melting transition with exponents $\alpha = 0.363(10), \beta = 0.089(8), \gamma = 1.448(24)$, and $\nu = 0.813(5)$, respectively. It is apparent that the latter transition belongs to a different universality class from the Ising transition.

ACKNOWLEDGMENTS

We would like to thank J. R. Lee for valuable discussions. This work was supported in part by the Ministry of Education, Republic of Korea through a grant to the Research Institute for Basic Sciences, Seoul National University and in part by the Korea Science Foundation through Research Grant to the Center for Theoretical Physics, Seoul National University.

[1] S. Teitel and C. Jayaprakash, Phys. Rev. B **27**, 598 (1983).
[2] D. B. Nicolaides, J. Phys. A **24**, L231 (1991).
[3] J. Lee, J. M. Kosterlitz, and E. Granato, Phys. Rev. B **43**, 11 531 (1991).
[4] G. Ramirez-Santiago and J. V. José, Phys. Rev. Lett. **68**, 1224 (1992).
[5] G. S. Grest, Phys. Rev. B **39**, 9267 (1989).
[6] J. R. Lee, Phys. Rev. B **49**, 3317 (1994).
[7] M. Yosefin and E. Domany, Phys. Rev. B **32**, 1778 (1985); M. Y. Choi and S. Doniach, Phys. Rev. B **31**, 4516 (1985).
[8] J. M. Kosterlitz and D. J. Thouless, J. Phys. C **6**, 1181 (1973).
[9] D. R. Nelson and J. M. Kosterlitz, Phys. Rev. Lett. **39**, 1201 (1977).
[10] P. Minnhagen, Phys. Rev. B **32**, 7548 (1985).
[11] J. Villain, J. Phys. C **10**, 1717 (1977); J. V. José, L. P. Kadanoff, S. Kirkpatrick, and D. R. Nelson, Phys. Rev. B **16**, 1217 (1977).
[12] K-C. Lee, J. Phys. A **23**, 2087 (1990).
[13] V. Privman and M. E. Fisher, Phys. Rev. B **30**, 322 (1984).
[14] K. Binder, Z. Phys. B **43**, 119 (1981).
[15] A. L. Scheinine, Phys. Rev. B **39**, 9368 (1989).
[16] P. Minnhagen, Phys. Rev. Lett. **54**, 2351 (1985).
[17] H. Weber and P. Minnhagen, Phys. Rev. B **37**, 5986 (1988).
[18] K-C. Lee, Phys. Rev. Lett. **69**, 9 (1992).